Highly selective Si₃N₄/SiO₂ etching using an NF₃/N₂/O₂/H₂ remote plasma. II. Surface reaction mechanism

Ji-Eun Jung,[1,a)] Yuri Barsukov,[1,a)] (ID) Vladimir Volynets,[1,a)] Gonjun Kim,[1,a)] Sang Ki Nam,[1,a)] Kyuhee Han,[1,a)] Shuo Huang,[2,b)] (ID) and Mark J. Kushner[2,c)] (ID)

AFFILIATIONS

[1]Mechatronics R&D Center, Samsung Electronics Co., Ltd., 1-1 Samsungjeonja-ro, Hwaseong-si, Gyeonggi-do 18448, South Korea
[2]Department of Electrical Engineering and Computer Science, University of Michigan, 1301 Beal Ave., Ann Arbor, Michigan 48109-2122

[a)]**Electronic addresses:** jieun.jung@samsung.com; barsukov.yuri@gmail.com; vladimir.volynets@samsung.com; gonjun.kim@samsung.com; sangki.j.nam@samsung.com; and khee.han@samsung.com
[b)]**Present address:** KLA Corp., 2550 Green Road, Suite 100, Ann Arbor, MI 48105. **Email:** shuo.huang@kla.com
[c)]**Electronic address:** mjkush@umich.edu

ABSTRACT

Developing processes for highly selective etching of silicon nitride (Si₃N₄) with respect to silicon dioxide (SiO₂) is a major priority for semiconductor fabrication processing. In this paper and in Paper I [Volynets *et al.*, J. Vac. Sci. Technol. A **38**, 023007 (2020)], mechanisms are discussed for highly selective Si₃N₄ etching in a remote plasma based on experimental and theoretical investigations. The Si₃N₄/SiO₂ etch selectivity of up to 380 was experimentally produced using a remote plasma sustained in NF₃/N₂/O₂/H₂ mixtures. A selectivity strongly depends on the flow rate of H₂, an effect attributed to the formation of HF molecules in vibrationally excited states that accelerate etching reactions. Based on experimental measurements and zero-dimensional plasma simulations, an analytical etching model was developed for etch rates as a function of process parameters. Reaction rates and sticking coefficients were provided by quantum chemistry models and also fitted to the experimental results. Etch rates from the analytical model show good agreement with the experimental results and demonstrate why certain etchants accelerate or inhibit the etch process. In particular, the modeling shows the important role of HF molecules in the first vibrationally excited state [HF($v = 1$)] in achieving high Si₃N₄/SiO₂ selectivity.

I. INTRODUCTION

As the aspect ratio of features in microelectronics fabrication increases, the need for higher selectivity during plasma etching becomes more acute. Developing processes for highly selective etching of silicon nitride (Si₃N₄) with respect to silicon dioxide (SiO₂) is now a critical step in the fabrication of 3D NAND memory.[1] Even though some wet etching techniques are able to achieve high selectivity,[2] plasma-based dry etching may be necessary for high aspect ratio features.[3] In developing such plasma-based processes, high energy ion bombardment that occurs when using conventional dry etching techniques can produce defects and degrade the quality of the structure.[4,5] To alleviate this damage, dry etching processes using remote plasma sources (RPS) are being developed, which isolate the wafer from energetic particle bombardment, including UV and VUV photons. Since there is no direct plasma exposure of the wafer in the process chamber, only neutral radicals act as etchants. Compared to direct plasma etching processes, isotropic and highly selective etching can be achieved for the proper choice of process conditions such as gas mixture composition, pressure, and RPS power.[1]

Achieving high selectivity for etching of Si₃N₄ over SiO₂ using RPS is ultimately related to the control of reactive fluxes to the substrate. Several gas mixtures such as CF₄/N₂/O₂ or NF₃/N₂/O₂ excited with RPS have produced a high Si₃N₄/SiO₂ selectivity.[1,6] The previous experiments[7] achieved a selectivity of 80 (the ratio of

the etch rate of Si_3N_4 compared to SiO_2) using an RPS sustained in NF_3/O_2 mixtures. In that process, we found that the main etchant was fluorine (F) atoms, while NO increases the rate of F migration on the Si_3N_4 surface during the etching process.

It has been shown that a solid by-product can be formed on the Si_3N_4 surface during plasma etching. Brewer and Miller reported that a blue film formed on silicon nitride during etching by CF_4/O_2 plasma.[8] Several studies later showed that the solid by-product that builds up during etching by fluorocarbon[9–13] and $NF_3/O_2/NH_3$ (Ref. 14) plasmas, which eventually inhibits the etching, is $(NH_4)_2SiF_6$ (ammonium fluorosilicate). $(NH_4)_2SiF_6$ is a relatively weakly bonded salt, which can be decomposed by heating into volatile species (NH_3, SiF_4, and HF). This volatility enables a cyclic process with an annealing step to be used to remove this layer and continue etching.[11–13]

Posseme et al. showed that a silicon nitride film modified by implantation by light ions can be selectively removed with respect to the nonmodified film.[15] H_2 plasma treatment modified the surface layer of silicon nitride, which enhanced its etch rate by liquid[15] and gaseous HF (Ref. 16) and by an NF_3/NH_3 remote plasma.[17] Sherpa et al. reported that silicon nitride etch rates by fluorinated (NF_3 or SF_6) plasmas can be enhanced by modifying the surface layer either by ion implantation[18] or by atomic hydrogen diffusion.[19]

After investigating remote plasma etching of Si_3N_4 and SiO_2 with NF_3/O_2 and $NF_3/N_2/O_2$ mixtures, we have conducted additional experiments using $NF_3/N_2/O_2/H_2$ mixtures with the goal of increasing selectivity using RPS. When varying the flow rate of H_2 in $NF_3/N_2/O_2/H_2$ through the RPS, the Si_3N_4/SiO_2 selectivity has a narrow peak with a maximum of around 380, which is about five times higher than that obtained in our previous investigation using NF_3/O_2 remote plasmas.[7] The experimental results are shown in Fig. 1. As is discussed in Paper I (Ref. 20), this peak of Si_3N_4/SiO_2 selectivity may be due to the production of the first vibrationally excited state of the HF molecule [HF ($v = 1$)], which is the most abundant excited state of HF for our process conditions according to zero-dimensional plasma simulations. Note that, although HF has been widely used in wet and dry etching of Si_3N_4, the possible importance of HF molecules in vibrationally excited states in the etching process has not previously been recognized.

Here, we discuss mechanisms for the selective etching of Si_3N_4 with respect to SiO_2 focusing on the role of HF($v = 1$) in this process. The experimental results (etch data and measured species densities at the wafer level), the description of the reaction mechanism for $NF_3/N_2/O_2/H_2$ plasmas, and the results of simulations of gas phase plasma chemistry are presented in Paper I (Ref. 20). In this paper, we propose a mechanism explaining the role of HF($v = 1$) in Si_3N_4 and SiO_2 etching based on the results of quantum chemistry modeling. An analytical etching model based on this mechanism was developed and validated with the experimental results.

II. QUANTUM CHEMISTRY MODELING OF ELEMENTARY ETCHING REACTIONS

Quantum chemistry modeling was performed using GAUSSIAN 16 (Ref. 21) to estimate the activation energies for the surface reactions
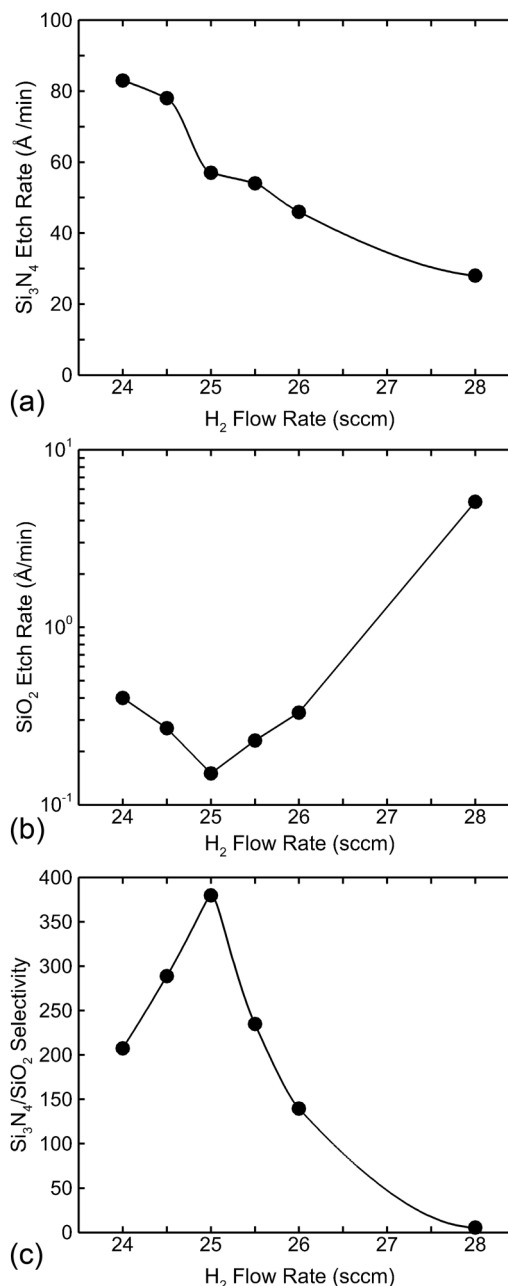

FIG. 1. Experimental results using $NF_3/N_2/O_2/H_2$ remote plasmas as a function of H_2 flow rate: (a) Si_3N_4 etch rate, (b) SiO_2 etch rate, and (c) etch selectivity of Si_3N_4/SiO_2.

of Si_3N_4 and SiO_2 with etchant radicals. As described in our previous work,[7] the use of clusters is justified due to the insulator properties and strongly localized electron density of Si_3N_4 and SiO_2. The basic cluster models, $Si_7N_8H_7F_{11}$ and $Si_8O_{12}H_3F_{11}$, that correspond to the initial surface sites of Si_3N_4 and SiO_2 are shown in Fig. 2. We

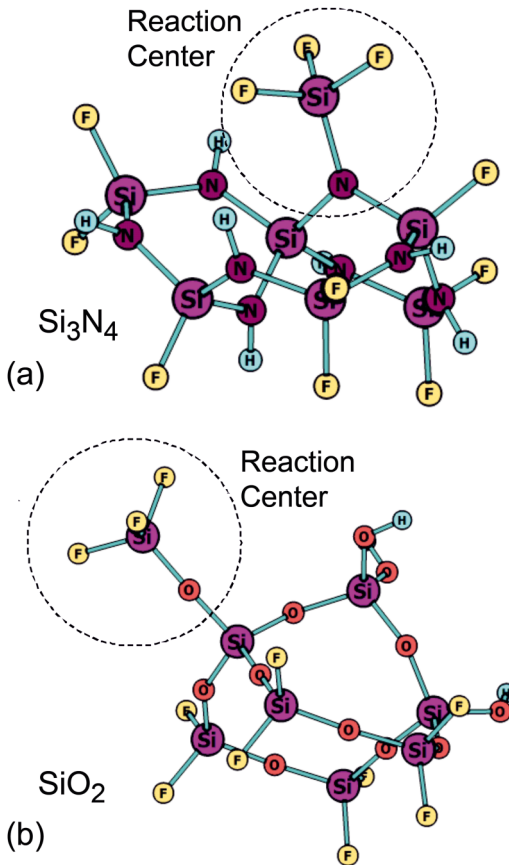FIG. 2. Cluster models used in the simulations: (a) $Si_7N_8H_7F_{11}$ and (b) $Si_8O_{12}H_3F_{11}$.

consider here only the surface sites, which are already strongly fluorinated, since we are focused on the reactions producing the final etch products, such as SiF_4. The surface fluorination is a natural result of high fluxes of F-atoms onto the wafer for our experimental conditions. The N–H and O–H bonds are formed by HF inserting into Si–N and Si–O bonds, so the vacancies on terminal N- and O-atoms in the clusters are closed by hydrogen atoms. The B3LYP hybrid functional using the 6–31 + G(d,p) basis set was used for all of the quantum chemistry calculations.

The $NF_3/N_2/O_2/H_2$ remote plasma produces HF, HF($v = 1$), H_2O, and F as the main etchants of both Si_3N_4 and SiO_2. We do not consider other species in the etching model that are potentially important, such as O, NO, H, OH, and FNO. Based on the modeling results discussed in Paper I (Ref. 20), the densities of OH and FNO are too low to make a meaningful contribution to etching. The densities of both O and NO have a weak dependence on the H_2 flow rate (FR), while the density of H has an almost linear increase as a function of H_2 FR. Given these dependencies, O, NO, and H would likely not produce a strong variation in etch rates and selectivity in a narrow range of H_2 FR, as shown in Fig. 1.

As discussed above, a solid surface by-product can be produced during the etching of Si_3N_4. During our experiments, this by-product was removed by an annealing step. The annealing step was not explicitly included in the model. We assumed that the by-product is fully converted into volatile etch products during the annealing step. Details of the etch model are discussed in Sec. III. In short, the etch model describes the beginning of the etching step when the solid by-product just starts to form and the surface is clean or partly clean. At this time, incident radicals can react directly with the substrate. Before the by-product builds up, we assume annealing will have been performed. Note that the by-product only applies to silicon nitride etching. No solid by-product is produced on the SiO_2 surface for our process conditions.

TABLE I. Reaction mechanism for Si_3N_4 or SiO_2 etching.

Sites		θ_1: initial Si_3N_4 or SiO_2 site; θ_{1a}: underlying Si_3N_4 or SiO_2 site; θ_2: HF adsorbed Si_3N_4 or SiO_2 site; θ_3: HF + HF($v = 1$) adsorbed Si_3N_4 or SiO_2 site; θ_4: HF + H_2O adsorbed Si_3N_4 or SiO_2 site; EP: etch product					
		S[a]		A (s^{-1})[b]		E_a/R (K)[b]	
	Reactions	Si_3N_4	SiO_2	Si_3N_4	SiO_2	Si_3N_4	SiO_2
R1	HF + $\theta_1 \rightarrow \theta_2$	1	1	—	—	—	—
R2	HF(v = 1) + $\theta_2 \rightarrow \theta_3$	1	1	—	—	—	—
R3	$\theta_2 \rightarrow$ HF + θ_1	—	—	8.2×10^8	3.0×10^{11}	2044	1996
R4	$\theta_3 \rightarrow$ 2HF + θ_1	—	—	2.1×10^9	8.0×10^{10}	3612	0
R5	H_2O + $\theta_2 \rightarrow \theta_4$	1	1	—	—	—	—
R6	$\theta_4 \rightarrow$ EP + θ_{1a}	—	—	1.18×10^{10}	1.46×10^{13}	7862	7399
R7	$\theta_3 \rightarrow$ EP + θ_{1a}	—	—	4.02×10^{11}	6.55×10^8	1756	8061
R8	H_2O + $\theta_3 \rightarrow \theta_4$ + HF	1	1	—	—	—	—
R9	F + $\theta_3 \rightarrow \theta_2$ + HF + F	0.086	0.086	—	—	—	—
R10	F + $\theta_1 \rightarrow$ EP + θ_{1a}	1.0×10^{-5}	0.5×10^{-5}	—	—	—	—

[a]S is the sticking coefficient for the adsorption of gas phase species on a surface site.
[b]Rate coefficient $k = A \exp(-(E_a/RT))$.

The elementary surface reactions in the mechanism are shown in Table I. The definitions of surface sites are

(1) θ_1: Initial Si_3N_4 or SiO_2 site;
(2) θ_{1a}: Underlying Si_3N_4 or SiO_2 site;
(3) θ_2: HF adsorbed Si_3N_4 or SiO_2 site;
(4) θ_3: HF + HF($v = 1$) adsorbed Si_3N_4 or SiO_2 site; and
(5) θ_4: HF + H_2O adsorbed Si_3N_4 or SiO_2 site.

In developing the etching mechanism, we assumed that the densities of surface sites are in the steady state. Reactive radicals produced by the plasma are adsorbed on the initial Si_3N_4 or SiO_2 surface sites, θ_1, or previously passivated sites producing radical-adsorbed-sites (RAS) such as θ_2, θ_3, or θ_4 (reactions R1, R2, R5, and R8 in Table I). Desorption occurs from the RAS producing the initial configuration of the surface (reactions R3 and R4 in Table I). Etching reactions produce gas phase products such as SiF_4, NH_3, HF, or H_2O, denoted by the etch product or EP in Table I, and expose an underlying Si_3N_4 or SiO_2 site, θ_{1a} (reactions R6, R7, and R10 in Table I). The underlying site θ_{1a} then functions the same as the initially pristine site, θ_1. In the etching mechanism, we also consider fluxes of HF molecules in the first vibrationally excited state [HF($v = 1$)]. These molecules participate in R2, where a second HF molecule adsorbs on an Si_3N_4 or SiO_2 RAS site, and in R7, where etching occurs due to the combined effect of the two adsorbed HF molecules, one being in the vibrationally excited state.

Rate coefficients for reaction i, k_i, were calculated in the Arrhenius form for the pre-exponential factor (A) and the activation energy (E_a),

$$k_i = A_i \exp\left(\frac{-E_{ai}}{RT}\right),$$ (1)

where R is the gas constant and T is the temperature (K). The values of activation energy (E_a) were calculated as the energy differences between the reactant and the transition state, which were found from the intrinsic reaction coordinate computation using the optimized reactant and product structures. All transition states (TS) were confirmed by the presence of one imaginary frequency from the saddle point in the reactant and product reaction paths. A statistical mechanical approach[22] was used for calculating the pre-exponential factor A for reactions R6 and R7,

$$A = \frac{k_B T}{h} \times \left(\frac{Q_{vib}^{TS}}{Q_{vib}^{Re}}\right),$$ (2)

where k_B, h, and T are Boltzmann's constant, Planck's constant, and temperature, respectively. Q_{vib}^{TS} and Q_{vib}^{Re} are the overall vibrational partition functions of the TS and the reagent complex, which were calculated by GAUSSIAN 16.[21]

The results of the quantum chemistry calculations are summarized in Table I. The activation energies are results of the calculations. The sticking coefficients and the pre-exponential factors of the desorption reactions (R3 and R4) were fitting parameters. When the elementary reaction is spontaneous and has zero activation energy, the sticking coefficient is $S = 1$. Otherwise, the sticking coefficients are fitted to reproduce the experimental results.

SiO_2 and Si_3N_4 are etched through reactions R6, R7, and R10 by HF + H_2O, HF + HF($v = 1$), and F, respectively. HF itself without any catalytic assist does not etch both Si_3N_4 and SiO_2 at room temperature. This inactivity results from HF having to overcome an energy barrier to dissociate and break Si–N or Si–O bonds. It was previously shown that a second adsorbed HF molecule or H_2O can significantly decrease this barrier and play the role of a catalyst. For example, Habuka et al.[23] experimentally studied the reactivity of HF with SiO_2 and showed that HF etches the surface at temperatures above 1000 K in the presence of water vapor. Hoshino et al.[24] investigated the mechanism for SiO_2 etching by HF using quantum chemistry modeling. They showed that the attack of the first Si–OH hydroxyl group by HF is the rate-limiting step. HF, HF($v = 1$), or H_2O can form a complex on the HF preadsorbed surface and catalyze etching. The role of water in the catalysis of SiO_2 etching by HF was investigated using quantum chemistry methods by Kang et al.[25] They found that the activation energy of the rate-limiting step for etching by the HF · H_2O complex is 22.1 kcal/mol (0.96 eV, 11 140 K) and by HF alone is 35.1 kcal/mol (1.52 eV, 17 639 K).

HF($v = 1$) can decrease the activation energy of the etching reaction by contributing about 0.5 eV (5800 K) of enthalpy to the system. However, this lowering of the activation energy occurs for Si_3N_4 but not for SiO_2. The vibrational quanta of the O–H and H–F bonds are close to each other, so HF($v = 1$) can quasiresonantly transfer its vibrational quantum to the OH group on the oxide surface. This quasiresonant transfer is functionally a two-step process. The first step, R1, is the formation of Si–OH groups upon the adsorption of HF onto SiO_2. The second step, R2, is the adsorption of HF($v = 1$) followed by the resonant transfer of vibrational energy to Si–OH. After this transfer, the quenched HF acts similarly to an initially adsorbed ground state HF having similar activation energy. At the same time, HF($v = 1$) quenching on a nitride surface should be much slower since there is no quasiresonant transfer of the vibrational quantum. If the reaction leading to Si–N bond breaking by the HF · HF($v = 1$) dimer is faster than the quenching process, HF($v = 1$) can play an important role in Si_3N_4 etching by lowering the activation energy barrier.

The adsorption of radicals on the surface is spontaneous without an activation barrier for both Si_3N_4 and SiO_2 (R1, R2, R5, and R9 in Table I). However, etching by reactions R6 and R7 is quite different for Si_3N_4 and SiO_2. When the surface is passivated by HF + H_2O, the activation energy for removing Si_3N_4 (7862 K) is slightly higher than for SiO_2 (7399 K) in reaction R6. On the other hand, with double adsorption of ground state HF, SiO_2 has a higher activation energy (8061 K) than Si_3N_4 (7556 K), based on our quantum chemistry calculations. As mentioned above, if the incident flux of HF contains vibrationally excited molecules, HF($v = 1$) contributes about 0.5 eV (5800 K) of enthalpy. HF($v = 1$) will be quenched on the SiO_2 surface, but, at the same time, it can lower the activation barrier in reaction R7 to 1756 K for Si_3N_4.

The end result is that etching of Si_3N_4 by HF + HF($v = 1$) has a low activation energy of 1756 K, while etching of SiO_2 by the same species has a higher activation energy of 8061 K. This difference in the activation energy produces a higher etch rate for Si_3N_4 compared to SiO_2 by reaction R7, which then results in a high Si_3N_4/SiO_2 selectivity. Note that etching of Si_3N_4 by HF + HF($v = 1$) is also related to reaction R4, desorption of HF from the

surface. HF molecules rapidly desorb from the SiO_2 surface without an activation energy. At the same time, HF molecules strongly stick to the Si_3N_4 surface with a binding energy of 3612 K against desorption, which increases the probability of etching reaction R7.

F-atoms are also etchants of both Si_3N_4 and SiO_2, whose sticking probabilities (S for R10) were estimated from our previous investigations using NF_3/O_2 mixtures.[7] Although both sticking coefficients are small, an order of 10^{-5}, with the F-atom flux being the highest of all the reactants, even these small reaction coefficients contribute to the etch reactivity of Si_3N_4 and SiO_2.

III. ANALYTICAL MODELING OF ETCH PROPERTIES

The results of the quantum chemistry modeling were incorporated into an analytical model to calculate etch rates. Based on the elementary etching reactions in Table I, the SiO_2 or Si_3N_4 etch model can be represented by

$$\frac{d\theta_1}{dt}\rho_s = -J_{HF}S_1\theta_1 + k_3\rho_s\theta_2 + k_4\rho_s\theta_3 + k_6\rho_s\theta_4 + k_7\rho_s\theta_3 = 0,$$

(3)

$$\frac{d\theta_2}{dt}\rho_s = J_{HF}S_1\theta_1 - J_{HF(v=1)}S_2\theta_2 - k_3\rho_s\theta_2 - J_{H_2O}S_5\theta_2 + J_F S_9\theta_3 = 0,$$

(4)

$$\frac{d\theta_3}{dt}\rho_s = J_{HF(v=1)}S_2\theta_2 - k_4\rho_s\theta_3 - k_7\rho_s\theta_3 - J_{H_2O}S_8\theta_3 - J_F S_9\theta_3 = 0,$$

(5)

$$\frac{d\theta_4}{dt}\rho_s = J_{H_2O}S_5\theta_2 - k_6\rho_s\theta_4 + J_{H_2O}S_8\theta_3 = 0,$$

(6)

$$\theta_1 + \theta_2 + \theta_3 + \theta_4 = 1,$$

(7)

where J_{HF}, $J_{HF(v=1)}$, J_{H2O}, and J_F are the fluxes of HF, HF($v=1$), H_2O, and F-atoms onto the wafer, respectively. These fluxes were derived from the gas phase plasma simulations discussed in Paper I (Ref. 20). The sticking coefficients are fitted to reproduce the experimental results.

The etch rate, ER, is proportional to the rates of reactions R6, R7, and R10 (see Table I),

$$ER = (k_6\theta_4\rho_s + k_7\theta_3\rho_s + J_F S_{10}\theta_1) \times \frac{M}{\rho N_A},$$

(8)

TABLE II. Constants used in the analytical model.

Constants	Value
M (Si_3N_4)	0.14 kg/mol
M (SiO_2)	0.06 kg/mol
ρ (Si_3N_4)	3200 kg/m^3
ρ (SiO_2)	2200 kg/m^3
ρ_s (Si_3N_4 and SiO_2)	1×10^{-5} mol/m^2

where M is the molar mass, ρ is the density of the etched material, ρ_s is the surface site density, and N_A is Avogadro's number. Constants used in the analytical model are in Table II.

As discussed above during etching, silicon nitride can be converted into a solid $(NH_4)_2SiF_6$ salt by gaseous HF after H_2 plasma treatment.[16] Hydrogen ion implantation activates the top Si_3N_4 layer, and the $(NH_4)_2SiF_6$ salt is formed on the surface by reactions with gas phase HF. If the $(NH_4)_2SiF_6$ layer exceeds a critical thickness, etching will terminate.[13] We assumed that the internal energy of vibrationally excited HF can be used for the activation of the surface reactions, which leads to transforming the top layer of Si_3N_4 into the $(NH_4)_2SiF_6$ salt. When this salt is produced, it is then fully converted into volatile etch products during the annealing step. Our etch model, therefore, describes the initial stage of the etching step (just after annealing and cooling) when the surface is at least partly clean, and species from the gas phase can freely react with the surface.

The simulated HF($v=1$) density in the process chamber has a narrow peak as a function of H_2 FR, as shown in Paper I (Ref. 20). HF($v=1$) is mainly produced by the reaction $F + H_2 \rightarrow HF$ ($v=1$) + H. The predicted density of F is sensitive to the surface recombination coefficients used in the model. These recombination coefficients depend on the state of the chamber wall, which is difficult to account for in the model.[4] Given uncertainties in the recombination coefficient, the experimental etch rate and selectivity data were slightly shifted as a function of the H_2 flow rate to align with the simulations.

The results from the analytical model and experimental data for Si_3N_4 and SiO_2 etch rates and etch selectivity are shown in Fig. 3. The model reproduces the experimental data quite well over the range of the available experimental data. The Si_3N_4 etch rate has a maximum near 21 sccm of H_2 flow, which corresponds to the local minimum in the SiO_2 etch rate. The result of these two trends is a sharp peak of Si_3N_4/SiO_2 etch selectivity around 21 sccm of H_2 flow.

Contributions of each etching reaction by F, HF + H_2O, and HF + HF($v=1$) to the total Si_3N_4 and SiO_2 etch rates as a function of the H_2 flow rate are shown in Fig. 4. The decreasing trend of Si_3N_4 etching by F (R10 in Table I) follows the flux of F-atoms onto the wafer as a function of the H_2 flow rate. With the increase in the H_2 flow rate, the reaction of F with H_2 depletes the F-atom density and flux. Contributions to Si_3N_4 etching by HF + HF($v=1$) (R7 in Table I) follow the flux of HF($v=1$). The flux of HF($v=1$) is highest around 21 sccm of the H_2 flow rate, where the gas phase densities of F and H_2 are approximately equal. It is at this flow rate that the contribution of HF($v=1$) to the etching is maximum. In Paper I (Ref. 20), it is shown that the H_2O production is low if the gas phase densities [H_2] < [F], and rapidly increases in case [H_2] > [F]. Therefore, etching of Si_3N_4 by the HF + H_2O mechanism (R6 in Table I) increases as soon as H_2O starts to be produced with H_2 flow rates over 21 sccm.

The simulated etch rate of SiO_2 decreases with H_2 flow rates below 21 sccm and increases for larger flow rates, as shown in Fig. 3(b). The main SiO_2 etchants are F-atoms for H_2 flow rates below 21 sccm and HF + H_2O for higher flow rates (i.e., etching by HF catalyzed by water[26]), as shown in Fig. 4(b). The most significant difference between the etching of Si_3N_4 and SiO_2 is that the
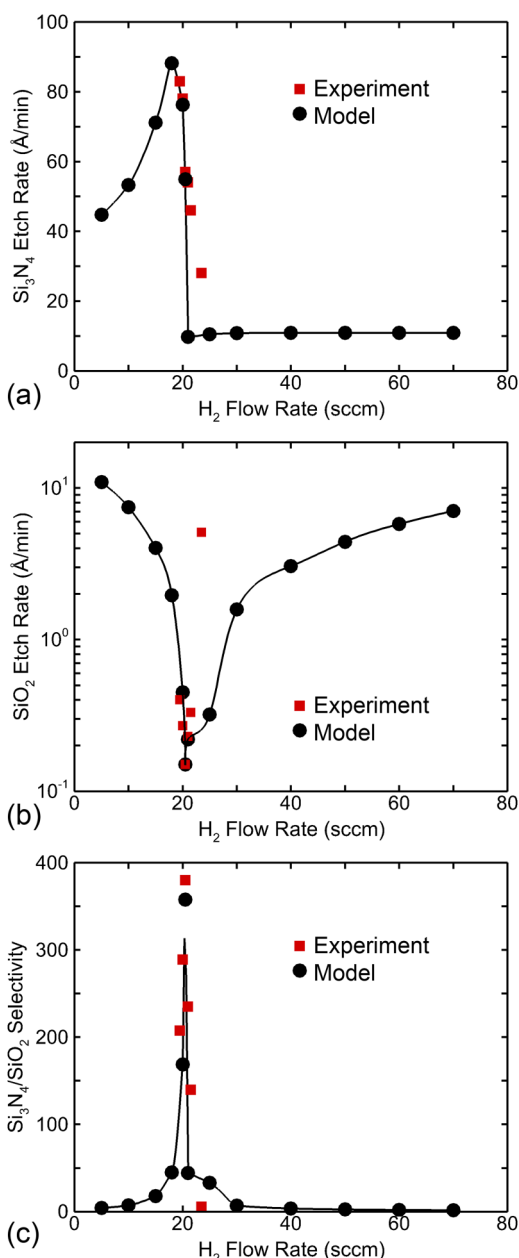
(a)

(b)

(c)

FIG. 3. Etch rate of Si_3N_4 and SiO_2 and etch selectivity as a function of the H_2 flow rate: (a) Si_3N_4 etch rate, (b) SiO_2 etch rate, and (c) etch selectivity of Si_3N_4/SiO_2.

(a)

(b)

FIG. 4. Separate contributions to the etch rate of Si_3N_4 and SiO_2: (a) Si_3N_4 etch rate and (b) SiO_2 etch rate.

and F than SiO_2, this is not sufficient to achieve high selectivity in the absence of $HF(v = 1)$. At the same time, our quantum chemistry modeling suggests that among the available reactants in $NF_3/N_2/O_2/H_2$ remote plasmas, only $HF(v = 1)$ is able to decrease the etching activation energy barrier for Si_3N_4 to a low value. The outcome of the combined experimental and modeling studies highlights the important role of HF in vibrationally excited states in highly selective Si_3N_4/SiO_2 etching.

IV. CONCLUDING REMARKS

Quantum chemistry and analytical modeling for the etching of Si_3N_4 and SiO_2 have been discussed for $NF_3/N_2/O_2/H_2$ remote plasmas as a function of the H_2 flow rate. The etch rates produced by the analytical model reproduce the experimental results, which show a high Si_3N_4/SiO_2 selectivity of up to 380. The flux of HF molecules in the first vibrationally excited state $[HF(v = 1)]$ plays an important role in achieving high selectivity by reducing the activation energy for reactions of HF with Si_3N_4. The reduction in activation energy enables the reaction with Si_3N_4 to have a lower activation energy barrier than with SiO_2. The reaction probability for etching by F-atoms is small for both Si_3N_4 and SiO_2; however,

contribution to SiO_2 etching by $HF + HF(v = 1)$ is near zero over the entire range of conditions investigated.

The sharp peak of Si_3N_4 etch rate and the near zero etch rate of SiO_2 by $HF + HF(v = 1)$ are the main reasons for the high etch selectivity of about 380 that occurs at an H_2 flow rate of 21 sccm. Note that even though Si_3N_4 has a higher etch rate by $HF + H_2O$
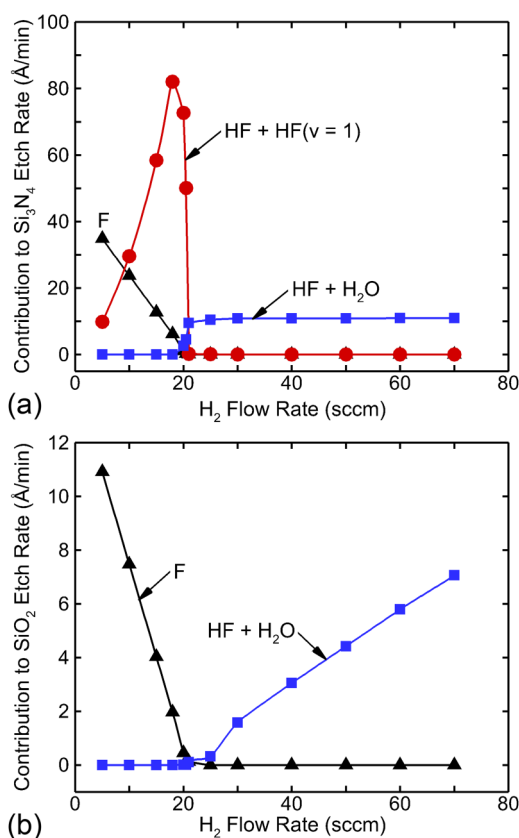
large fluxes of F-atoms produce a finite contribution to etching. Process conditions that produce large fluxes of $HF(v = 1)$ while minimizing fluxes of F, as can be achieved in $NF_3/N_2/O_2/H_2$ remote plasma sources, maximize the Si_3N_4/SiO_2 etch selectivity.

ACKNOWLEDGEMENTS

REFERENCES

[1]B. E. E. Kastenmeier, P. J. Matsuo, and G. S. Oehrlein, J. Vac. Sci. Technol. A **17**, 3179 (1999).

[2]Y.-H. C. Chien, C.-C. Hu, and C.-M. Yang, J. Electrochem. Soc. **165**, H3187 (2018).

[3]B. Wu, A. Kumar, and S. Pamarthy, J. Appl. Phys. **108**, 051101 (2010).

[4]V. M. Donelly and A. Kornblit, J. Vac. Sci. Technol. A **31**, 050825 (2013).

[5]K. J. Kanarik, T. Lill, E. A. Hudson, S. Sriraman, S. Tan, J. Marks, V. Vahedi, and R. A. Gottscho, J. Vac. Sci. Technol. A **33**, 020802 (2015).

[6]B. E. E. Kastenmeier, P. J. Matsuo, G. S. Oehrlein, and J. G. Langan, J. Vac. Sci. Technol. A **16**, 2047 (1998).

[7]Y. Barsukov, V. Volynets, S. Lee, G. Kim, B. Lee, S. K. Nam, and K. Han, J. Vac. Sci. Technol. A **35**, 061320 (2017).

[8]J. A. Brewer and G. W. Miller, J. Vac. Sci. Technol. B **1**, 932 (1983).

[9]W. R. Knolle and R. D. Huttemann, J. Electrochem. Soc. **135**, 2574 (1988).

[10]Y. Kataoka, Sh. Saito, and K. Omiya, J. Electrochem. Soc. **146**, 3435 (1999).

[11]K. Shinoda, M. Izawa, T. Kanekiyo, K. Ishikawa, and M. Hori, Appl. Phys. Express **9**, 106201 (2016).

[12]N. Miyoshi, H. Kobayashi, K. Shinoda, M. Kurihara, T. Watanabe, Y. Kouzuma, K. Yokogawa, S. Sakai, and M. Izawa, Jpn. J. Appl. Phys. **56**, 06HB01 (2017).

[13]K. Shinoda, N. Miyoshi, H. Kobayashi, M. Izawa, T. Saeki, K. Ishikawa, and M. Hori, J. Vac. Sci. Technol. A **37**, 051002 (2019).

[14]Y. Wang and L. Luo, J. Vac. Sci. Technol. A **16**, 1582 (1998).

[15]N. Posseme, O. Pollet, and S. Barnola, Appl. Phys. Lett. **105**, 051605 (2014).

[16]V. Ah-Leung, O. Pollet, N. Posseme, M. Garcia-Barros, N. Rochat, C. Guedj, G. Audoit, and S. Barnola, J. Vac. Sci. Technol. A **35**, 021408 (2017).

[17]N. Posseme, A. Ah-Leung, O. Pollet, C. Arvet, and M. Garcia-Barros, J. Vac. Sci. Technol. A **34**, 061301 (2016).

[18]S. D. Sherpa and A. Ranjan, J. Vac. Sci. Technol. A **35**, 01A102 (2017).

[19]S. D. Sherpa, P. L. G. Ventzek, and A. Ranjan, J. Vac. Sci. Technol. A **35**, 05C310 (2017).

[20]V. Volynets, Y. Barsukov, G. Kim, J.-E. Jung, S.-Ki Nam, K. Han, S. Huang and M. J. Kushner, J. Vac. Sci. Technol. A **38**, 023007 (2020).

[21]M. J. Frisch et al., GAUSSIAN 16, Revision B.01, Gaussian, Inc., Wallingford, CT, 2016.

[22]D. A. McQuarrie and J. D. Simon, Physical Chemistry: A Molecular Approach (University Science Book, Sausalito, CA, 1997).

[23]H. Habuka and T. Otsuka, Jpn. J. Appl. Phys. **37**, 6123 (1998).

[24]T. Hoshino and Y. Nishioka, J. Chem. Phys. **111**, 2109 (1999).

[25]J. K. Kang and C. B. Musgrave, J. Chem. Phys. **116**, 275 (2002).

[26]C. R. Helms and B. E. Deal, J. Vac. Sci. Technol. A **10**, 806 (1992).